



OPEN

Utilization of the peroxidase-like activity of silver nanoparticles nanozyme on *O*-phenylenediamine/ H_2O_2 system for fluorescence detection of mercury (II) ions

Mohamed A. Abdel-Lateef

Polyvinylpyrrolidone stabilized silver nanoparticles (PV-AgNPs) were synthesized from $AgNO_3$ /trisodium citrate and with the assistance of microwave energy. The synthesized PV-AgNPs were found to own an actual peroxidase mimicking activity. This catalytic activity can oxidize the non-fluorescence reagent (*o*-phenylenediamine) to a high fluorescence reaction product (2,3-diaminophenazine). The reaction product exhibited a fluorescence emission at 563 nm upon the excitation at 420. Among many metals, only mercury (II) ions can inhibit the catalytic activity of PV-AgNPs nanozyme. Accordingly, the fluorescence intensity of the reaction product has been successfully quenched. This quenching effect in the fluorescence intensity was directly proportional to the concentration of mercury (II). Depending on this finding, a simple, cost-effective, and selective spectrofluorimetric approach has been designed for mercury (II) detection in water samples. The linear relationship between the inhibition in fluorescence intensity and mercury (II) concentration was found in 20–2000 nM with a detection limit of 8.9 nM.

Mercury metal is one of the most known poisonous and widely spread heavy metals due to its harmful effects upon accumulation in the human body¹. It is widely distributed in the soil, atmosphere, and seawater through human activities and natural phenomena, causing serious results on most living organisms and the environment². The main contamination sources by mercury (II) for surface waters and wastewater are Chlor-alkali production, paper and pulp, oil refinery, batteries, and paint manufacturing processes in industries³. Due to its high affinity for thiol groups found in enzymes and proteins, mercury can accumulate in human body tissues and vital organs, producing toxic and damaging human health even in low quantities⁴. Some chronic and acute symptoms and signs generated by the inorganic mercury toxicity are as follows: mouth inflammation; thirst; metallic taste; nausea; excessive salivation; kidney degeneration, and tremor⁵.

The selectivity and the sensitivity of the utilized chemosensory for detecting mercury (II) ion in water samples is an essential demand. Therefore, the utilized sensor should be characterized by simplicity, low cost, high sensitivity, and adequate selectivity, which can be sensing mercury (II) ions in aqueous samples at the nanomolar level and without interferences from the presences of other metals ions.

Nanoparticles are widely applied as sensors for detecting environmental pollutants^{6–9}. Many researchers are interested in silver nanoparticles due to their unusual optical features, SPR band, and ultrasmall size^{10–13}. Silver nanoparticles are also widely employed in the sensor, textile industries, and food storage due to their excellent conductivity and catalytic activity^{10–15}. The distinctive, unique enzyme-like activity of metals nanoparticles has attracted interest in the catalysis of numerous chemical reactions and metals analysis applications¹⁶.

There are many merits for using nanoparticles as an enzyme mimics/artificial enzyme over natural enzymes that focus on the absence of the inherent hindrances of the natural enzyme. These hindrances include time-consuming, tedious, availability of the natural resources and expensive purification process; sensitivity towards the elevated temperatures, rigorous storage conditions, sensitivity for the alkaline and the acidic pH conditions and proteases, leading to decreased stability lowering the shelf life^{17,18}. Enzyme mimics inorganic nanoparticles

Department of Pharmaceutical Analytical Chemistry, Faculty of Pharmacy, Al-Azhar University, Assiut Branch, Assiut 71524, Egypt. email: mohamed_abdellateef@azhar.edu.eg

are afforded with some features, including low cost, high stability, resistance to the high concentrations of the substrate, ease of storage process, and ease of synthesis^{19–21}.

In general, nanoparticles of noble metals (such as gold, silver, platinum, and palladium) exhibit appealing physicochemical features that are dependent on their form and size^{6,16}. For example, the peroxidase-like catalytic activity of gold nanoparticles has been utilized for the colorimetric sensing of mercury (II) and lead ions in water samples^{22,23}. Furthermore, the catalytic activity of platinum nanoparticles has been utilized to detect mercury (II) ions in water samples^{24,25}. Also, the catalytic activity of silver nanoparticles has been employed for visual colorimetric detection of protein and as a resonance Rayleigh scattering sensor for mercury (II) ions detection^{26–28}. The catalytic activity of these nanomaterials depends on their sizes, known as the “size effect”; for instance, the great catalytic activity for gold nanoparticles can be observed with nano sizes smaller than 5.0 nm^{16,29,30}. For that reason, a lot of efforts have been devoted to reducing the size of the synthesized nanoparticles³¹.

The reported studies prove that using polyvinylpyrrolidone surfactant to prepare Ag-NPs produces tiny nano sizes below 10 nm and stabilizes the formed nanoparticles for a long period^{32,33}. Furthermore, microwave irradiation energy over conventional heating causes uniform and rapid heating to the solution. It thus produces homogeneous nucleation sites in the solution and growth conditions, causing monodispersed nanoparticles in a short time³⁴. Moreover, microwave irradiation can be afforded good particle size distribution and smaller particle sizes to synthesize silver nanoparticles³⁵.

Fluorescence spectrometer is a highly sensitive analytical technique that usually offers great selectivity without losing precision^{36–38}. Designing a fluorescent sensor for mercury (II) ions detection relying on the peroxidase-like property of silver nanoparticles has not been investigated yet. Therefore, this work aims to use the catalytic activity of the smaller size polyvinylpyrrolidone stabilized silver nanoparticles as a nanozyme for the fluorescence detection of mercury (II) ions.

Materials, instruments, and methods

Materials. *O*-Phenylenediamine, polyvinylpyrrolidone, and silver nitrate have been produced by Sigma-Aldrich Chemical Co (Steinheim, Germany).

Aluminum nitrate, barium chloride, cadmium chloride, chromium chloride, cobalt nitrate, calcium chloride, magnesium chloride, hydrogen peroxide, mercuric chloride, nickel nitrate, sodium chloride, potassium chloride, and zinc nitrate have been produced by El-Nasr chemical Co. (Cairo, Egypt). Trisodium citrate has been produced by Fisher Scientific Co. (Leicestershire, UK). Ultrapure water was utilized in all experimental steps.

Instruments. The fluorescence spectra were performed on an FS2 fluorescent spectrometer (Scinco, Korea). The morphology of the prepared silver nanoparticles has been characterized by JSM 5400 LV SEM (JEOL, Tokyo, Japan). The nano size, polydispersion index, and the quality of the prepared silver nanoparticles have been characterized by ZEN 1690 (Malvern Instruments, Malvern, UK). SM-2000MW microwave oven (Smart Co., China) was utilized for heating process.

Synthesis of silver nanoparticles using microwave energy. 0.2% w/v PVP solution, 10 mM trisodium citrate solution and 10 mM silver nitrate solution were simultaneously poured into a 250 mL flask in the ratio of 0.5:1:1 and mixed by magnetic stirring for 3 min. The flask has been heated for about 12 min at 90 °C by microwave irradiation. The formation of polyvinylpyrrolidone silver nanoparticles (PVP-AgNPs) can be evidenced by the transformation of the colorless solution to a yellowish-green colloidal state.

Detection of mercury (II) ion. In a series of calibrated flasks (10 mL), suitable volumes of mercury (II) solutions (in the range of 100 nM to 20 μM) and 800 μL of PVP-AgNPs solution were poured, incubated for 2 min and followed by the addition of 800 μL from *O*-phenylenediamine (prepared by dissolving 0.108 g in 100 mL water) solution. Then, 400 μL of 3% w/v hydrogen peroxide solution was added into the content, and the content was vortexed for 1 min. After incubation for 15 min at room temperature, the volume has been completed to a 10-mL by deionized water. The blank solution has been simultaneously prepared by the same steps with omitting the addition of mercury (II) solution. The quenching in the fluorescence intensity of the blank solution upon the addition mercury (II) was measured at the $\lambda_{\text{emission}}$ of 563 nm, upon the $\lambda_{\text{excitation}}$ of 420 nm. The specificity of the suggested method has been checked by the addition of different metal ions solutions at the concentration of 10 μM instead of mercury (II) ion in the abovementioned procedures.

Detection of mercury (II) in different water samples using PVP-AgNPs. Tap water and bottled water samples were collected from our laboratory and a local establishment. The collected samples were spiked with different known concentrations of mercury (II). Then after, the water samples were filtered utilizing a 0.45 μm syringe filter to discard any particulates matter. Finally, the abovementioned general analytical assay was followed.

Results and discussion

Characterization and peroxidase mimicking activity of PVP-AgNPs. The morphology and elemental characteristics [particle size, polydispersity index (PDI), size uniform] of PVP-AgNPs were examined using SEM device and zeta-sizer device, respectively. Figure 1 shows the SEM image of PVP-AgNPs, which refers to the spherical-rod-like shape of the synthesized nanomaterial. The measured size of the synthesized PVP-AgNPs was 5.5 nm with uniform size, good quality, and a low polydispersity index value of 0.440 Fig. 1A. The size of nanoparticles is the main factor responsible for their catalytic activity³⁹. Generally, the catalytic per-

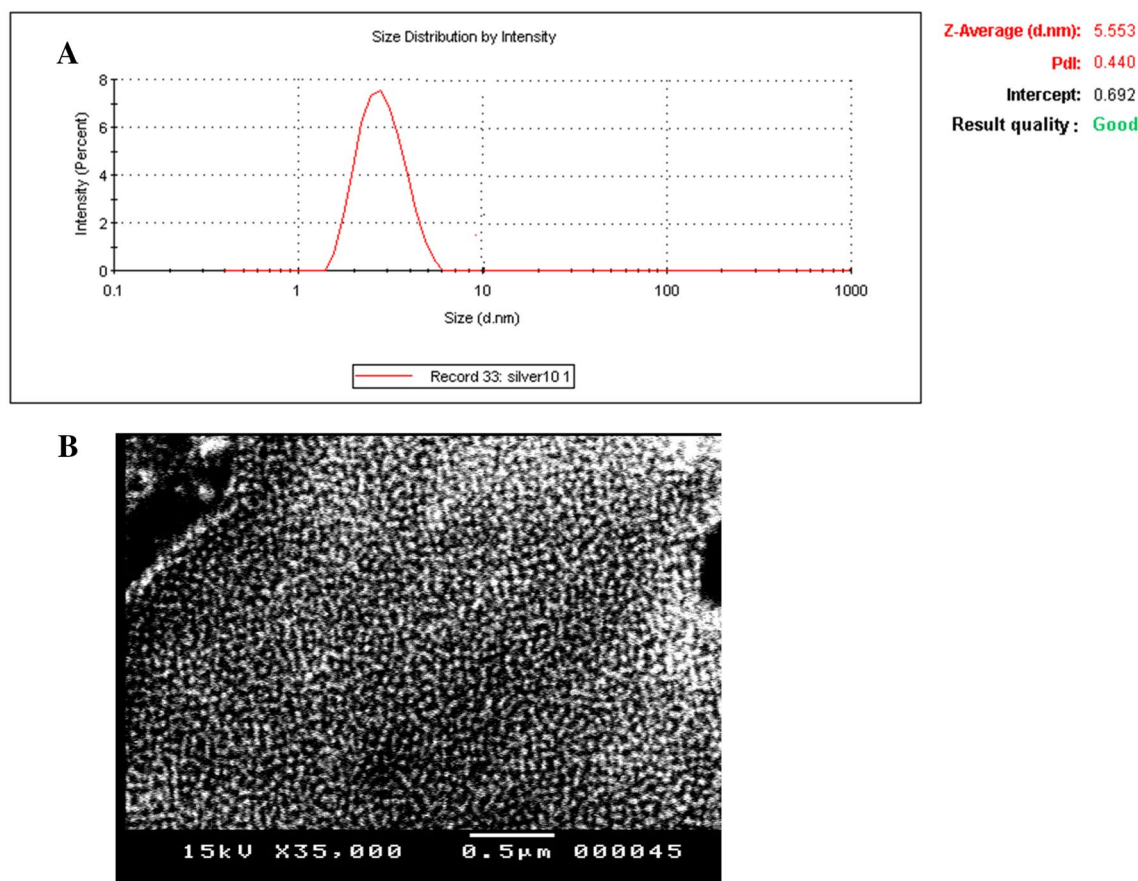


Figure 1. (A) Characterization size, PDI value and quality of the synthesized PVP Ag-NPs by zeta-sizer device; (B) Characterization of the morphology of the synthesized PVP Ag-NPs by SEM device.

formance of the silver nanoparticles is inversely proportional to the nanosize of their particles⁴⁰. In the current study, the determined size of the prepared PVP-AgNPs is very small (5.5 nm), which refers to their superior catalytic activity.

O-Phenylenediamine (OPD) is one of the typical substrates utilized to investigate the peroxidase-like activity of the nanoparticles^{25,41}. OPD (colorless and non-fluorescent) has been oxidized by peroxidase mimicking activity of certain nanoparticles to 2,3-phenazinediamine (colored and fluorescent)²⁵. Herein, the peroxidase mimicking activity of the prepared PVP-AgNPs has been examined by the fluorescence technique and the spectrophotometric technique using OPD/H₂O₂ system. Practically, the catalytic activity of the prepared PVP-AgNPs has been spectrophotometrically confirmed by the appearance of characteristic absorbance peak at $\lambda_{\text{max}} = 420$ nm, Fig. 2. Furthermore, it has been fluorometrically evidenced by the existence of a distinct fluorescence peak at $\lambda_{\text{emission}} = 563$ upon $\lambda_{\text{excitation}} = 420$, Fig. 2. Moreover, it was found that only the mixture of PVP-AgNPs/OPD/H₂O₂ exhibited this fluorescence behavior. In contrast, neither one of the PVP-AgNPs/OPD mixture, OPD/H₂O₂ mixture, and PVP-AgNPs/H₂O₂ mixture has produced any fluorescence character at the same conditions. These absorbance peak and fluorescence emission peak values are matching to those of 2,3-phenazinediamine that were reported in studies of literature²⁵.

Fabrication and design of mercury (II) fluorescence detection sensing system. It is well known that the colored 2,3-phenazinediamine, which possesses a distinctive fluorescent behavior at $\lambda_{\text{emission}} = 563$ nm/ $\lambda_{\text{excitation}} = 420$ nm, is the oxidized product of o-phenylenediamine. Initially, the colorless solution changed from non-fluorescent to a bright fluorescence yellow solution when the PVP-AgNPs were added to the o-phenylenediamine/H₂O₂ system. In this reaction, the prepared PVP-AgNPs owned peroxidase mimicking activity that can catalyze the oxidation of o-phenylenediamine with H₂O₂ to yield 2,3-phenazinediamine as the main reaction product.

Mercury has a unique advantage over the rest of the elements through its ability to form an amalgam with certain elements such as gold, platinum, and silver^{24,25,27,28,42,43}. Therefore, in this study, the formation of Ag-Hg amalgam produces an effective inhibition for the catalytic activity of PVP-AgNPs, combined with changing their surface properties. This catalytic inhibition effect of PVP-AgNPs prevents the transformation of the OPD/H₂O₂ system to 2,3-phenazinediamine. Accordingly, a quenching action on the fluorescence intensity of the solution upon the addition of mercury (II) in comparison with the fluorescence intensity of blank sample (without Hg²⁺),

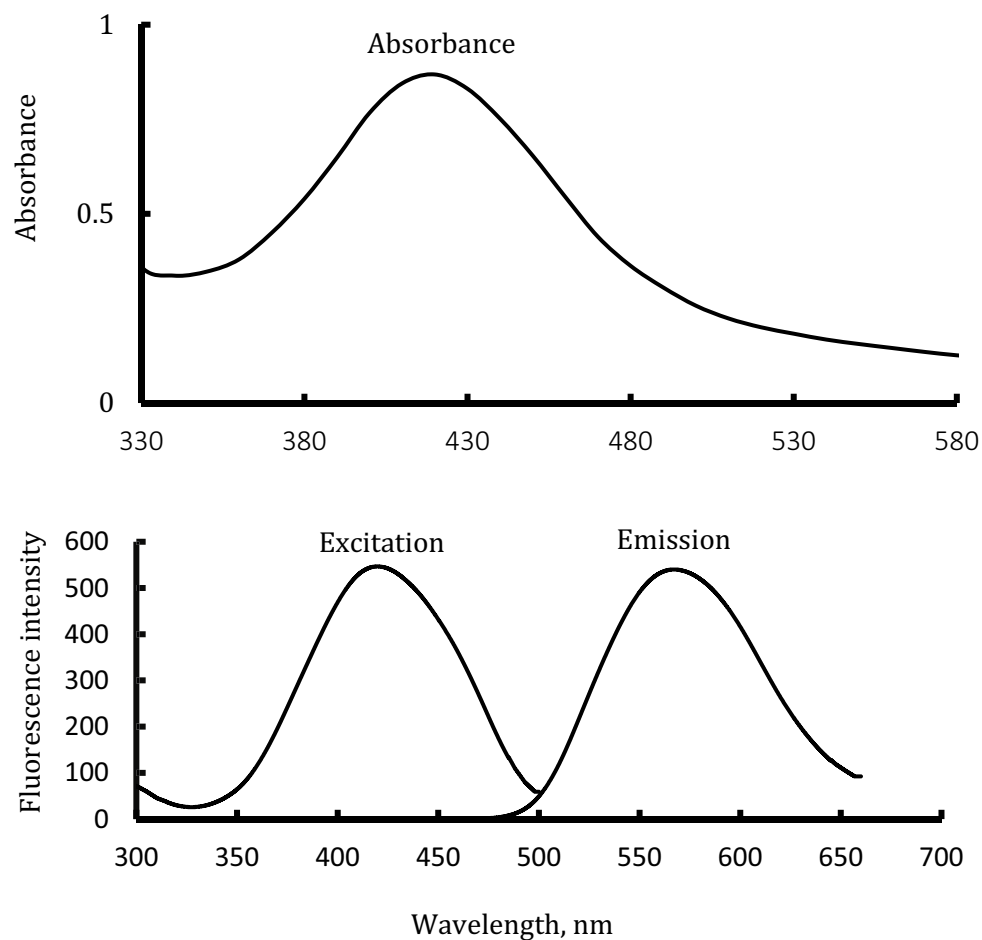


Figure 2. Examining the peroxidase mimicking activity for the prepared PVP-Ag-NPs by forming the characterized absorption and fluorescence (excitation/emission) spectra of OPDA reaction product (2,3-phenazinediamine).

Fig. 3. Therefore, the selective determination of mercury (II) in a certain linear concentration range was achieved. The sensing mechanism of mercury (II) is illustrated in Scheme 1.

Optimization of the sensing system and fluorescent readout assay of mercury (II). The reaction conditions involved the volume of H_2O_2 , reaction time, the volume of OPDA, and the volume of PVP-Ag-NPs were examined and optimized to find the optimum conditions for analysis. The sensing system was incubated with mercury (II) for 15 min and the optimum conditions for the quenching in the fluorescence intensity of the solution (in compared to the blank solution) was obtained with 800 μL of PVP-AgNPs suspension, 800 μL of OPD solution, and 400 μL of 3% w/v hydrogen peroxide solution, Fig. 4. This quenching effect in the fluorescence intensity of the solution is directly proportional with the concentration of mercury (II).

The linear relationship between the quenching of fluorescence emission at 563 nm and mercury (II) concentration was established in the ranging of 20 nM to 2 μM with the regression equation of $y = 0.1352x + 13.51$, R^2 value of 0.998, and LOD value of 8.9 nM ($S/N = 3$, where N represents noise and S represents sensitivity). The statistical parameters for detecting Hg^{2+} by the fluorescence methodology are presented in Table 1. Other common metals such as Al^{3+} , Ba^{2+} , Ca^{2+} , Cd^{2+} , Co^{2+} , Cr^{3+} , K^+ , Mg^{2+} , Ni^{2+} , Na^+ , and Zn^{2+} have been tested by the current fluorescent methodology to investigate the selectivity of the design sensing system. It was found that there is no obvious effect in the emission intensity of PVP-AgNPs/OPD/ H_2O_2 system have been detected upon adding of any metals from mentioned metals at higher concentration level (tenfold excess in compared to mercury (II)). In contrast, the emission intensity of PVP-AgNPs/OPD/ H_2O_2 has been significantly decreased in the presence of mercury (II) which refers to the good selectivity for the fabricated system (Fig. 5). The explanation for the perfect selectivity of the proposed method for mercury (II) may be attributed to the formation of Ag-Hg amalgam through a specific interaction between silver nanoparticles and mercury (II) ion⁴².

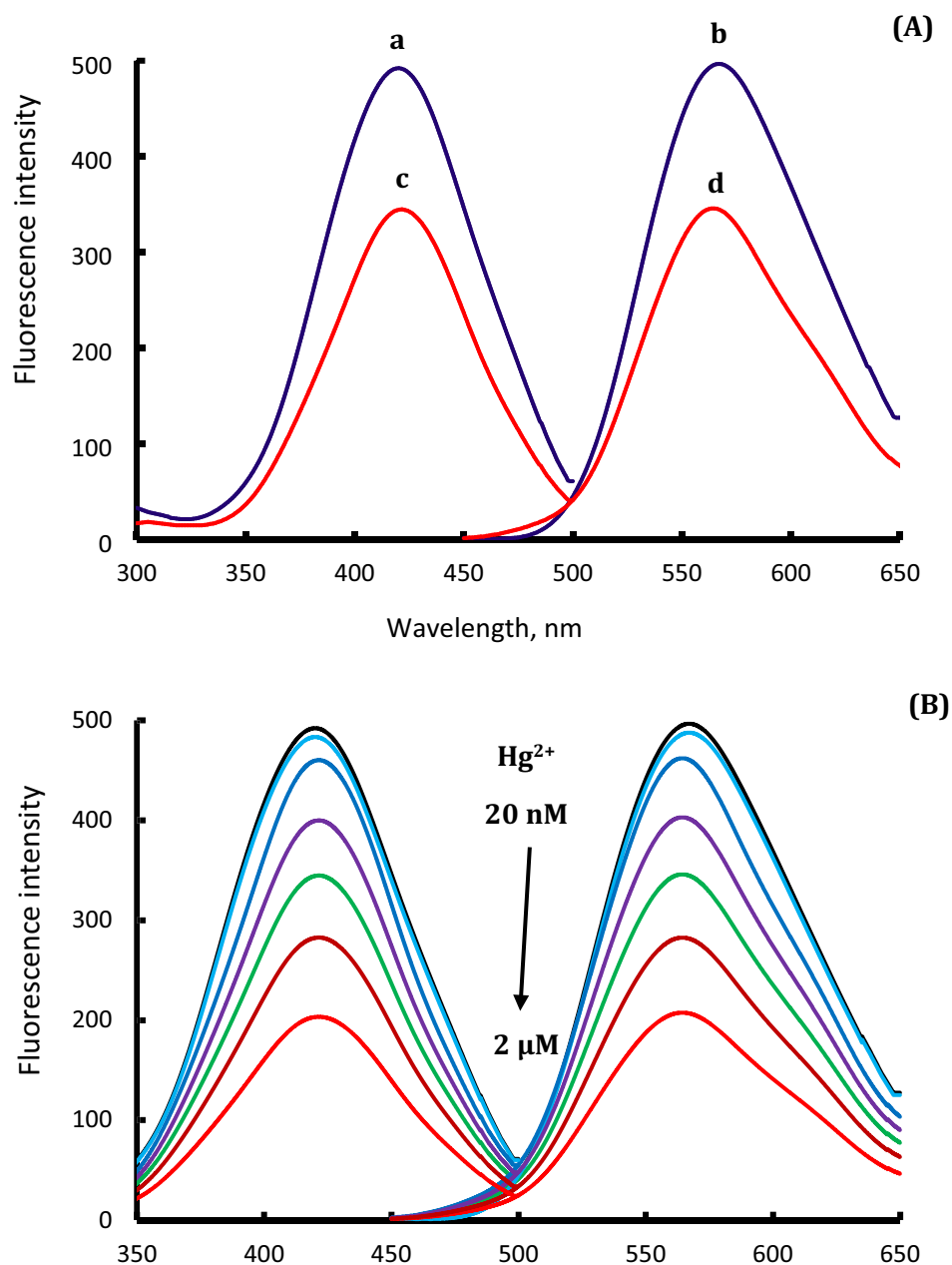
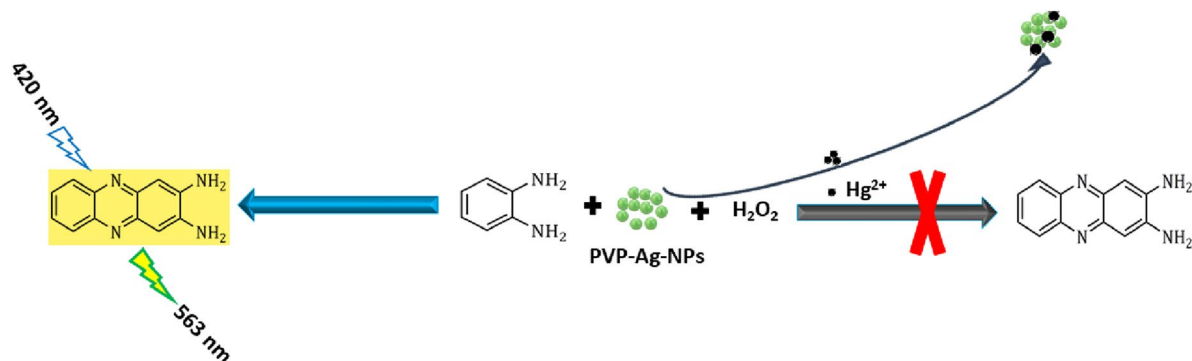


Figure 3. (A) for fluorescence (excitation and emission) spectra of OPD/ H_2O_2 /PVP-Ag-NPs system (a, b, respectively) and after their quenching by $1.0 \mu\text{M}$ of Hg^{2+} (c, d), while (B) for fluorescence spectra of OPD/ H_2O_2 /PVP-Ag-NPs system in the presence of various concentrations of Hg^{2+} .

Fluorescence detection of mercury (II) ions in tap and bottled water samples. The applications of PVP-AgNPs for spiked samples experiments were performed with tap water samples and bottled water samples. To evaluate the practicality for applying the fluorescent methodology in tap water samples and bottled water samples have been spiked with mercury (II) at different concentration levels and tested by the suggested methodology. The data in Table 2 refers to the good recovery and SD values for determining mercury (II) ions by the current method. These SD and recovery values evidenced the validity of accuracy and precision of the presented methodology for mercury (II) detection in tap water samples and bottled water samples.

Conclusions

In this study, the microwave irradiation energy was utilized to assist the synthesis of polyvinylpyrrolidone stabilized silver nanoparticles with very small nano sizes. The prepared silver nanoparticles showed distinctive peroxidase activity behavior. Based on the inhibition effect of mercuric (II) ions towards this peroxidase activity of the prepared silver nanoparticles, a fluorescent methodology with a highly sensitive and extremely selective



Scheme 1. Schematic elucidation for the detection of mercury (II) by spectrofluorimetric technique.

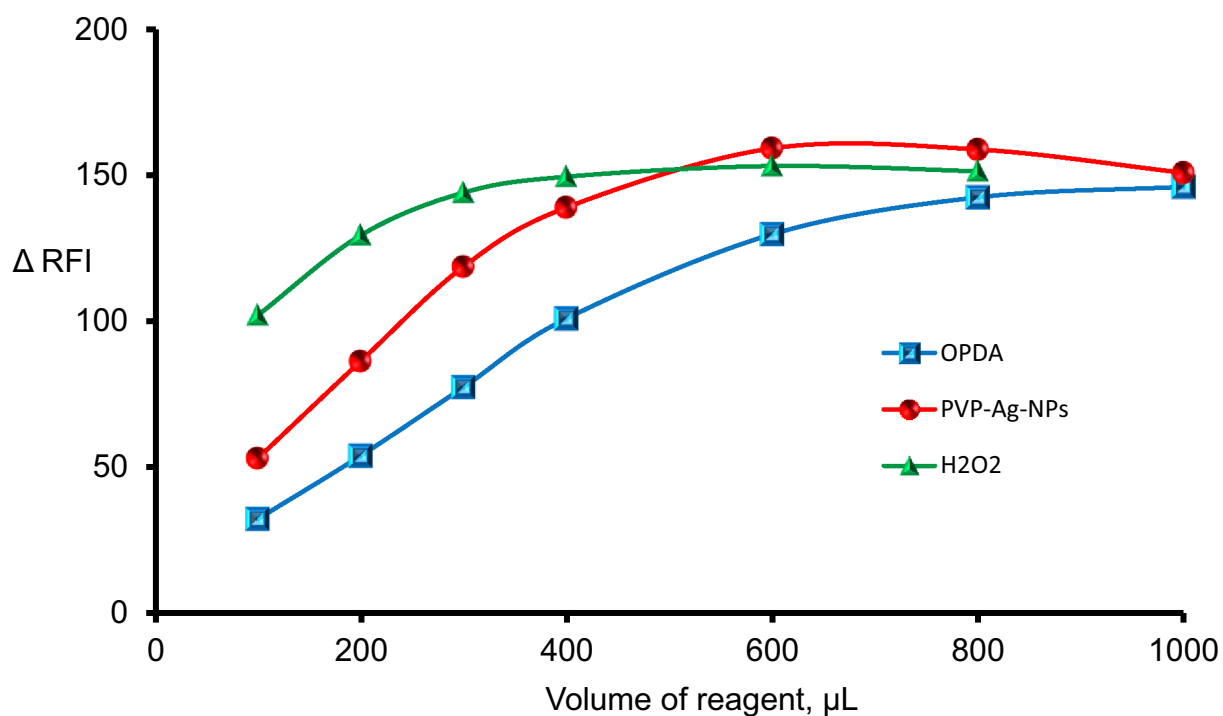


Figure 4. Investigating the volume of reagents for Hg^{2+} (1.0 μM) detection by the suggested method.

Parameter	Spectrofluorimetric assay
Linear range (nM)	20–2000
Standard error	5.41
Intercept	13.35
Standard error of intercept	3.42
Slope	0.1353
Standard error of slope	0.003
Correlation coefficients (r)	0.9989
Determination coefficients (r^2)	0.9979
Number of determinations	6

Table 1. Analytical parameters for the proposed fluorescence method.

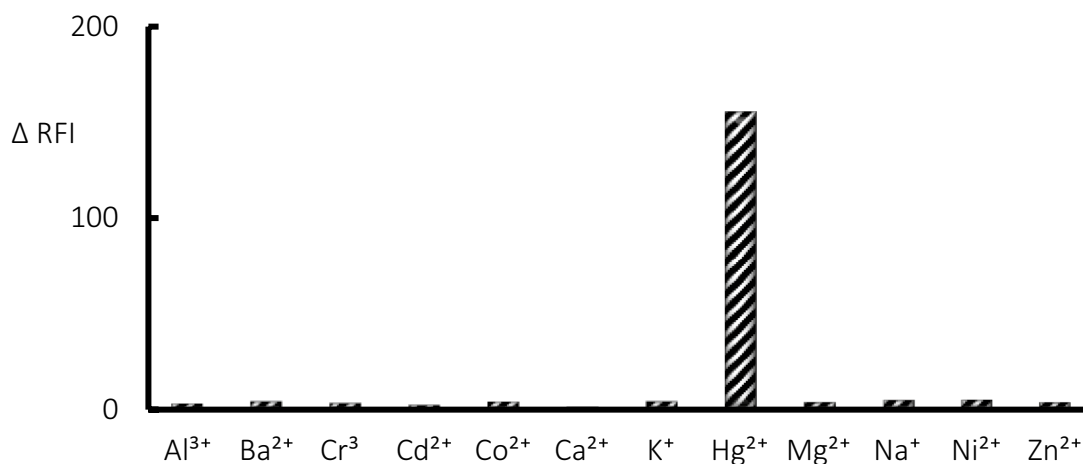


Figure 5. Examining the selectivity of the utilized system (OPD + H₂O₂ + PVP-Ag-NPs) for the detection of Hg²⁺ ion (1 μM) in the presence of common metals ions (10 μM).

Sample	Added Hg ²⁺ (nM)	Found Hg ²⁺ (nM)	Recovery ± SD
Tap water	500	510.54	102.11 ± 1.54
Tap water	1000	979.38	97.94 ± 2.22
Tap water	2000	2057.48	102.87 ± 2.21
Bottled water	500	513.75	102.75 ± 2.08
Bottled water	1000	1013.38	101.34 ± 1.97
Bottled water	2000	1980.61	99.03 ± 2.04

Table 2. Results for the detection of mercury (II) in tap and bottled water samples.

response towards mercuric (II) ions detection was established. Under the optimum conditions, the provided assay exhibited a detection limit (LOD) of 8.9 nM with a linear range of 20–2000 nM. The current methodology proffered some advantages regarding to the greenness of synthesis, tiny particle size, good stability, and uniformity, using smaller concentration from the nanozyme, and easiness of the detection.

Received: 18 January 2022; Accepted: 11 April 2022

Published online: 28 April 2022

References

- Clarkson, T. W., Magos, L. & Myers, G. J. The toxicology of mercury—Current exposures and clinical manifestations. *N. Engl. J. Med.* **349**(18), 1731–1737 (2003).
- Boening, D. W. Ecological effects, transport, and fate of mercury: A general review. *Chemosphere* **40**(12), 1335–1351 (2000).
- Parham, H., Zargar, B. & Shiralipour, R. Fast and efficient removal of mercury from water samples using magnetic iron oxide nanoparticles modified with 2-mercaptobenzothiazole. *J. Hazard. Mater.* **205**, 94–100 (2012).
- Zhao, M. *et al.* A reaction-type receptor for the multi-feature detection of Hg²⁺ in water and living cells. *N. J. Chem.* **44**(29), 12538–12545 (2020).
- D’Mello, J. F. *Food Safety: Contaminants and Toxins* (CABI, 2003).
- Balasurya, S. *et al.* Rapid colorimetric detection of mercury using silver nanoparticles in the presence of methionine. *Spectrochim. Acta. A. Mol. Biomol. Spectrosc.* **228**, 117712 (2020).
- Lee, K.-S. & El-Sayed, M. A. Gold and silver nanoparticles in sensing and imaging: Sensitivity of plasmon response to size, shape, and metal composition. *J. Phys. Chem. B* **110**(39), 19220–19225 (2006).
- Pomal, N. C. *et al.* Functionalized silver nanoparticles as colorimetric and fluorimetric sensor for environmentally toxic mercury ions: An overview. *J. Fluoresc.* **31**(3), 635–649 (2021).
- Bhatt, K. D. *et al.* Turn-on fluorescence probe for selective detection of Hg (II) by calixpyrrole hydrazide reduced silver nanoparticle: Application to real water sample. *Chin. Chem. Lett.* **27**(5), 731–737 (2016).
- Maruthupandi, M., Chandhru, M., Rani, S. K. & Vasimalai, N. Highly selective detection of iodide in biological, food, and environmental samples using polymer-capped silver nanoparticles: Preparation of a paper-based testing kit for on-site monitoring. *ACS Omega* **4**(7), 11372–11379 (2019).
- Chandhru, M., Logesh, R., Kutti Rani, S., Ahmed, N., Vasimalai, N. Green synthesis of silver nanoparticles from plant latex and their antibacterial and photocatalytic studies. *Environ. Technol.* <https://doi.org/10.1080/09593330.2021.1914181> (2021).
- Eswaran, S. G. *et al.* Preparation of a portable calorimetry kit and one-step spectrophotometric nanomolar level detection of L-Histidine in serum and urine samples using sebamic acid capped silver nanoparticles. *J. Sci. Adv. Mater.* **6**(1), 100–107 (2021).
- Maruthupandi, M. & Vasimalai, N. Nanomolar detection of L-cysteine and Cu²⁺ ions based on Trehalose capped silver nanoparticles. *Microchem. J.* **161**, 105782 (2021).
- Chandhru, M., Rani, S. K. & Vasimalai, N. Reductive degradation of toxic six dyes in industrial wastewater using diamino benzoic acid capped silver nanoparticles. *J. Environ. Chem. Eng.* **8**(5), 104225 (2020).

15. Eswaran, S. G., Narayan, H. & Vasimalai, N. Reductive photocatalytic degradation of toxic aniline blue dye using green synthesized banyan aerial root extract derived silver nanoparticles. *Biocatal. Agric. Biotechnol.* **36**, 102140 (2021).
16. Sun, Z. *et al.* High-throughput colorimetric assays for mercury (II) in blood and wastewater based on the mercury-stimulated catalytic activity of small silver nanoparticles in a temperature-switchable gelatin matrix. *Chem. Commun.* **50**(65), 9196–9199 (2014).
17. Deng, H.-H. *et al.* Colorimetric sensor based on dual-functional gold nanoparticles: Analyte-recognition and peroxidase-like activity. *Food Chem.* **147**, 257–261 (2014).
18. Dutta, A. K. *et al.* CuS nanoparticles as a mimic peroxidase for colorimetric estimation of human blood glucose level. *Talanta* **107**, 361–367 (2013).
19. Gao, L. *et al.* Intrinsic peroxidase-like activity of ferromagnetic nanoparticles. *Nat. Nanotechnol.* **2**(9), 577–583 (2007).
20. Hu, L. *et al.* Copper nanoclusters as peroxidase mimetics and their applications to H₂O₂ and glucose detection. *Anal. Chim. Acta* **762**, 83–86 (2013).
21. Xie, J. *et al.* Co₃O₄-reduced graphene oxide nanocomposite as an effective peroxidase mimetic and its application in visual biosensing of glucose. *Anal. Chim. Acta* **796**, 92–100 (2013).
22. Li, W. *et al.* Fabrication of a covalent organic framework and its gold nanoparticle hybrids as stable mimetic peroxidase for sensitive and selective colorimetric detection of mercury in water samples. *Talanta* **204**, 224–228 (2019).
23. Chen, X. *et al.* Colorimetric detection of Hg²⁺ and Pb²⁺ based on peroxidase-like activity of graphene oxide–gold nanohybrids. *Anal. Methods* **7**(5), 1951–1957 (2015).
24. Kora, A. J. & Rastogi, L. Peroxidase activity of biogenic platinum nanoparticles: A colorimetric probe towards selective detection of mercuric ions in water samples. *Sens. Actuators B Chem.* **254**, 690–700 (2018).
25. Zhou, Y. & Ma, Z. Fluorescent and colorimetric dual detection of mercury (II) by H₂O₂ oxidation of o-phenylenediamine using Pt nanoparticles as the catalyst. *Sens. Actuators B Chem.* **249**, 53–58 (2017).
26. Liu, L., Zhang, L. & Liang, Y. A simple visual strategy for protein detection based on oxidase-like activity of silver nanoparticles. *Food Anal. Methods* **14**, 1–8 (2021).
27. Wang, G.-L., Zhu, X.-Y., Jiao, H.-J., Dong, Y.-M. & Li, Z.-J. Ultrasensitive and dual functional colorimetric sensors for mercury (II) ions and hydrogen peroxide based on catalytic reduction property of silver nanoparticles. *Biosens. Bioelectron.* **31**(1), 337–342 (2012).
28. Al-Onazi, W. A. & Abdel-Lateef, M. A. Catalytic oxidation of O-phenylenediamine by silver nanoparticles for resonance Rayleigh scattering detection of mercury (II) in water samples. *Spectrochim. Acta A Mol. Biomol. Spectrosc.* **264**, 120258 (2022).
29. Lee, S., Fan, C., Wu, T. & Anderson, S. L. CO oxidation on Au n/TiO₂ catalysts produced by size-selected cluster deposition. *J. Am. Chem. Soc.* **126**(18), 5682–5683 (2004).
30. Bamwenda, G. R., Tsubota, S., Nakamura, T. & Haruta, M. The influence of the preparation methods on the catalytic activity of platinum and gold supported on TiO₂ for CO oxidation. *Catal. Lett.* **44**(1), 83–87 (1997).
31. Wang, X.-X., Wu, Q., Shan, Z. & Huang, Q.-M. BSA-stabilized Au clusters as peroxidase mimetics for use in xanthine detection. *Biosens. Bioelectron.* **26**(8), 3614–3619 (2011).
32. Dang, T. M. D., Le, T. T. T., Fribourg-Blanc, E. & Dang, M. C. Influence of surfactant on the preparation of silver nanoparticles by polyol method. *Adv. Nat. Sci. Nanosci. Nanotechnol.* **3**(3), 035004 (2012).
33. Huang, W., Zhang, L., Yang, Q. & Wang, Z. Polyvinylpyrrolidone as an efficient stabilizer for silver nanoparticles. *Chin. J. Chem.* **32**(9), 909–913 (2014).
34. Nadagouda, M. N., Speth, T. F. & Varma, R. S. Microwave-assisted green synthesis of silver nanostructures. *Acc. Chem. Res.* **44**(7), 469–478 (2011).
35. Sreeram, K. J., Nidhin, M. & Nair, B. U. Microwave assisted template synthesis of silver nanoparticles. *Bull. Mater. Sci.* **31**(7), 937–942 (2008).
36. Abdel-Lateef, M. A., Ali, R., Omar, M. A. & Derayea, S. M. Micellar-based spectrofluorimetric method for the selective determination of ledipasvir in the presence of sofosbuvir: Application to dosage forms and human plasma. *Luminescence* **35**(4), 486–492 (2020).
37. Abdel-Lateef, M. A. & Almahri, A. Spectrofluorimetric determination of α -difluoromethylornithine through condensation with ninhydrin and phenylacetaldehyde: Application to pharmaceutical cream and spiked urine samples. *Chem. Pap.* **76**, 741–748 (2022).
38. Abdel-Lateef, M. A. & Almahri, A. Micellar sensitized Resonance Rayleigh Scattering and spectrofluorometric methods based on isoindole formation for determination of Eflornithine in cream and biological samples. *Spectrochim. Acta A Mol. Biomol. Spectrosc.* **258**, 119806 (2021).
39. Cao, S., Tao, F. F., Tang, Y., Li, Y. & Yu, J. Size- and shape-dependent catalytic performances of oxidation and reduction reactions on nanocatalysts. *Chem. Soc. Rev.* **45**(17), 4747–4765 (2016).
40. Panáček, A. *et al.* Polyacrylate-assisted size control of silver nanoparticles and their catalytic activity. *Chem. Mater.* **26**(3), 1332–1339 (2014).
41. Lian, J. *et al.* Core-shell structured Ag-CoO nanoparticles with superior peroxidase-like activity for colorimetric sensing hydrogen peroxide and o-phenylenediamine. *Colloids Surf. A Physicochem. Eng. Aspects* **603**, 125283 (2020).
42. Deng, L. *et al.* Exploiting the higher specificity of silver amalgamation: Selective detection of mercury (II) by forming Ag/Hg amalgam. *Anal. Chem.* **85**(18), 8594–8600 (2013).
43. Rastogi, L., Sashidhar, R., Karunasagar, D. & Arunachalam, J. Gum kondagogu reduced/stabilized silver nanoparticles as direct colorimetric sensor for the sensitive detection of Hg²⁺ in aqueous system. *Talanta* **118**, 111–117 (2014).

Author contributions

The manuscript was prepared by M.A.-L.

Funding

Open access funding provided by The Science, Technology & Innovation Funding Authority (STDF) in cooperation with The Egyptian Knowledge Bank (EKB).

Competing interests

The author declares no competing interests.

Additional information

Correspondence and requests for materials should be addressed to M.A.A.-L.

Reprints and permissions information is available at www.nature.com/reprints.

Publisher's note Springer Nature remains neutral with regard to jurisdictional claims in published maps and institutional affiliations.



Open Access This article is licensed under a Creative Commons Attribution 4.0 International License, which permits use, sharing, adaptation, distribution and reproduction in any medium or format, as long as you give appropriate credit to the original author(s) and the source, provide a link to the Creative Commons licence, and indicate if changes were made. The images or other third party material in this article are included in the article's Creative Commons licence, unless indicated otherwise in a credit line to the material. If material is not included in the article's Creative Commons licence and your intended use is not permitted by statutory regulation or exceeds the permitted use, you will need to obtain permission directly from the copyright holder. To view a copy of this licence, visit <http://creativecommons.org/licenses/by/4.0/>.

© The Author(s) 2022